European Commission

HORIZON 2020

GUIDANCE DOCUMENTS ON MEASUREMENTS & MODELLING OF NOVEL AIR QUALITY POLLUTANTS:

BLACK CARBON (BC) DETERMINATIONS

RI URBANS

RI-URBANS

Research Infrastructures Services Reinforcing Air Quality Monitoring Capacities in European Urban & Industrial AreaS (GA n. 101036245)

By

CSIC Consejo Superior de Investigaciones Científicas

University of Helsinki

Joint Research Centre JRC

INERIS

30/10/2024

RI-URBANS (http://www.RIURBANS.eu) is supported by the European Commission under the Horizon 2020 – Research and Innovation Framework Programme, H2020-GD-2020, Grant Agreement number: 101036245

Authors: Marjan Savadkoohi (CSIC), Marco Pandolfi (CSIC), Andres Alastuey (CSIC), Tuukka Petäjä (UHEL), Jean Philippe Putaud (JRC), Olivier Favez (INERIS), Xavier Querol (CSIC)

Reviewers: Hilkka Timonen (FMI), Karri Saarnio (FMI), Katriina Kyllönen (FMI), Elli Suhonen (FMI), Christoph Hüglin (EMPA)

RI-URBANS (http://www.RIURBANS.eu) is supported by the European Commission under the Horizon 2020 – Research and Innovation Framework Programme, H2020-GD-2020, Grant Agreement number: 101036245

Table of Contents

ABBREVIATIONS

ACTRIS	Aerosols, Clouds and Trace gases Research InfraStructure
ACTRIS - CAIS	ACTRIS Centre for Aerosol in-Situ Measurements
ACTRIS - ECAC	ACTRIS European Center for Aerosol Calibration and Characterization
AE	Aethalometer
AQ	Air quality
b_{abs}	Absorption coefficient
b_{ATN}	Attenuation of light
BC	Black carbon
CEN	European Committee for Standardization
C_0	Constant that depends on the filter tape used
D	Deliverable
EAQP	European Air Quality Portal from the European Environmental Agency (EEA)
EBAS	A database infrastructure developed and operated by Norwegian Institute for Air Research, with datasets from EMEP, ACTRIS, GAW, among others
eBC	Equivalent black carbon
EC	Elemental carbon
EMEP	European Monitoring and Evaluation Programme
EN	European standard
EU	European Union
FAP	Filter absorption photometers
GAW	Global Atmospheric Watch programme by WMO
H*	Standardized harmonization factor provided by ACTRIS
M	Milestone
MAAP	Multi angle absorption photometer
MAC	Mass absorption cross-section
NAQD	New European Air Quality Directive (formally adopted 14th October 2024)
OC	Organic carbon
PM	Particulate matter
PM_{10}	Mass concentration of particles <10 µm
$PM_{2.5}$	Mass concentration of particles <2.5 µm
QA/QC	Quality assurance and quality control
RB	Regional background
RI-URBANS	Research Infrastructures Services Reinforcing Air Quality Monitoring Capacities in European Urban & Industrial AreaS EU-project
SSA	Single scattering albedo
SOP	Standard operation procedure

SUB	Sub-urban background
TR	Traffic
TS	Technical specifications
UB	Urban background
UFP	Ultrafine particle(s)
WHO	World Health Organization
WMO	World Meteorological Organization

CHEMICAL SPECIES

NO_2	Nitrogen dioxide

1 ABOUT THIS DOCUMENT

This document was prepared as part of the "Research Infrastructures Services Reinforcing Air Quality (AQ) Monitoring Capacities in European Urban & Industrial AreaS" (RI-URBANS) EU-project that connects the atmospheric observation expertise from Aerosols, Clouds and Trace gases Research InfraStructure (ACTRIS) with the urban air quality observation capacities of the regulatory air quality monitoring networks. It is specifically connected to the new European AQ Directive (NAQD) adopted on 14th October 2024.

The NAQD underlines the importance of emerging pollutants for AQ and the well-being of the citizens. Particularly, novel pollutants such as ultrafine particles (UFP), UFP-number size distribution (PNSD), black carbon (BC) and elemental carbon (EC), as well as ammonia (NH_3) and numerous volatile organic compounds (VOCs), and measurements of tracers of potential toxicity of PM (oxidative potential (OP) of particulate matter PM), are required or recommended to be monitored at both rural and urban supersites in order to support scientific understanding of their effects on health and the environment.

In order to ensure that the measurements on air pollution are sufficiently representative and comparable across Europe, it is important that standardized measurement techniques and common criteria for the number and location of measuring stations are used for the assessment of ambient air quality. The aim of this document is to facilitate upscaling of measurement methods for BC within air quality monitoring networks. We provide an up-to-date summary of the methodologies related to BC particles, summarize recent scientific synthesis of Pan-European observations and provide concise recommendations on the determination of BC in urban environments.

This is a RI-URBANS/ACTRIS guidance for this specific service tool that is part of the RI-URBANS deliverable D46 (D6.1, containing guidance for all service tools provided in the project) with the support for publication from AXA Research Fund to build up the final dissemination D55 (D7.6). Any dissemination of results must indicate that it reflects only the author's view and that the European Commission is not responsible for any use that may be made of the information it contains.

2 DEFINITION OF BLACK CARBON (BC)

The NAQD defines 'black carbon' (BC) as a carbonaceous aerosol measured by its light absorption. We provide hereafter methodologies for deriving BC concentrations from optical measurements. However, the agreement on terminology including all aspects definitions, determination methods, and uncertainties of BC is highly challenging.

The terms elemental carbon (EC) and black carbon (BC) are commonly used to refer to the most refractory, insoluble and strongly light-absorbing components of PM, mainly emitted by incomplete combustion of fossil fuels and biomass. **EC and BC are both defined by the respective determination method**, primarily addressing thermal refractoriness and light absorption, respectively. Note that there is a CEN standard for the thermo-optical measurement of EC in PM2.5 (EN16909:2017). The particle light absorption coefficient (b_{abs}) can be measured or retrieved from optical measurements by means of filter absorption photometers (FAPs). Black carbon mass concentrations (µg m^{-3}) can only be indirectly inferred from b_{abs} (m^{-1}) data by applying a conversion factor called the mass absorption cross-section (MAC, m^2 g^{-1}).

When reporting results on equivalent BC mass concentrations derived from optical methods, the term equivalent BC (eBC), recommended by Petzold et al. (2013), has generally been used by the scientific community. The attribute "equivalent" signifies that the actual concentration of light absorbing PM is equivalent (in terms of light absorption) to that mass concentration of eBC characterised by that MAC value. Thus, FAPs actually provide eBC concentrations, based on manufacturer-defined MAC values, which are obtained by comparing EC and b_{abs}. Such eBC concentrations are nothing else than b_{abs} values (m^{-1}) expressed in another unit (µg m^{-3}). The MAC value can also be obtained by calibrating eBC measurements in situ (in the measurement site/supersite) using data from collocated EC filter measurements, and in this case the BC will reflect the EC concentration. Following recommendations by Savadkoohi et al. (2024) we will use thereafter the term eBC for the mass concentration estimated from b_{abs} regardless of which MAC is used for eBC calculation.

3 MEASUREMENT METHODS FOR DETERMINING eBC

The measurements of eBC mass concentrations are commonly performed using FAPs. Widely used FAPs are the Aethalometer (AE) and the multi angle absorption photometer (MAAP). The MAAP instrument production was discontinued, and the AEs are now the most deployed instrument for eBC determination. There are other instruments that can be used to determine eBC from measurement of b_{abs} but nowadays they are less deployed. Moreover, there are other instruments based on photoacoustic techniques and on interferometry that are less used for air quality monitoring purposes.

3.1 State of harmonisationand relevant guidance

Currently there are no CEN standards or similar guidelines for determination of eBC. However, there are several initiatives to evaluate the standardization of BC or eBC mass concentrations using online methods, primarily FAPs. These initiatives include:

- CEN Working Group WG35.
- European Partnership on Metrology Project StanBC: (Standardization of Black Carbon Aerosol Metrics for Air Quality and Climate Modelling, https://stanbc.com/).
- So-called "ACTRIS eBC working group" established in the frame of the CAMS21a contract with ECMWF.

A number of technical guidance documents and reports are then available for measuring b_{abs} using FAPs. Notably, documents prepared by Global Atmosphere Watch (GAW) and ACTRIS provide comprehensive recommendations, guidelines, standard operating procedures, and scientific articles for aerosol in-situ measurements including aerosol inlets and conditioning (recommendations for aerosol drying, aerosol inlets and sampling tubes), instrument operation, quality assurance/quality control (QA/QC), and data management (data recording and data evaluation). These resources are openly available at the Measurement Guidelines - CAIS-ECAC (actris-ecac.eu). Some of these guidelines are related to eBC determination are listed in the "Reference" section.

GAW recommendations are available. There is also an ACTRIS guideline for Manual QC of MAAP and AE33.

We also provide here a selection of publications providing recommendations for reporting eBC and describing the different techniques/instruments, these are: Muller et al. (2011), Petzold et al. (2013), Drinovec et al. (2015), and Savadkoohi et al. (2024).

3.2 Sampling and conditioning

The following recommendations are available from ACTRIS CAIS-ECAC, European Centre for Aerosol Calibration and Characterization: https://www.actris-ecac.eu/actris-gaw-recommendation-documents.html.

3.2.1 Sampling

The measuring instruments should be housed in a protected environment under controlled conditions (temperature 20 °C to 30 °C). To measure aerosols in air quality, the air inlet must be generally between 1.5 m and 4 m above the ground (2008/50/CE, 2015/1480/CE). A PM_{10} inlet should be generally used. This cut-off is harmonized with the WMO-GAW network. The NAQD states that *'higher siting may also be appropriate if the sampling point is located in a background location; the decision to apply such higher siting shall be fully documented'*. This NAQD also sets lower level at 0.5 m. But for most AQ measurements 1.5 m is selected.

It is necessary to minimize diffusional losses for ultrafine particles, and losses due to impaction and sedimentation for super-micrometre particles. To this end, sampling tubes shall be as short as possible, avoiding bends and horizontal pipes. Sampling tubes should be made of a conductive, corrosion-resistant material with a low surface roughness (e.g., stainless steel).

FAPs can be connected to a single dedicated inlet or to common inlet through an isokinetic splitter. The inlet and the flow-splitter shall be checked regularly to detect obstructions and cleaned, if necessary. We describe here some simple settings for AEs that can be changed by the user. Other relevant guidance is reported elsewhere.

AEs usually work at a flow rate of 5 L/min. Lower vales as 2 L/min can be used at measurement sites where the signal received by the instrument is high (i.e. high BC concentrations). However, a flow of 5 L/min is recommended.

eBC mass concentrations provided by FAPs are reported at specific standard temperature and pressure (STP) conditions. ACTRIS requires reporting data at standard conditions (T_0=273 K, P_0=1013.25 hPa). It is recommended to measure ambient pressure and temperature. If T_{ref} and P_{ref} are the T and P set in the AE software for reporting eBC, then the following equation can be used to report the eBC mass concentrations at other P and T conditions (Eq. 1).

$$(1)\quad eBC = eBC_{ref} \cdot \left(\frac{P_{ref}}{P}\right) \cdot \left(\frac{T}{T_{ref}}\right)$$

3.2.2 Drying

The aerosol in-situ measurements should be done at a relative humidity lower than 40%. This is necessary to obtain comparable data, given that the size of hygroscopic particles is highly influenced by humidity. Different methods can be employed to achieve a relative humidity (RH) below 40%. Drying of aerosol samples using single tube Nafion© dryers is recommended in GAW/ACTRIS. Different Nafion© dryer designs are available for low flow rates (~1 L/min) and larger flow rates (up to ~8 L/min).

For FAPs instrument, the relative humidity, temperature, and pressure should be measured. RH should be measured in the inlet before and after the Nafion© dryer.

3.3 Determination of eBC

Determination of eBC concentrations using FAPs is done in two steps. In the first step is the absorption coefficient (b_{abs}) is measured. In the second step b_{abs} is converted into eBC concentrations assuming a given Mass Absorption

Cross Section (MAC) of BC particles. In this section we will describe the principle of measurement of the b_{abs} and eBC.

3.3.1 Measurement of absorption

The attenuation or transmission of light through the sample spot is continuously recorded by the instrument. When exceeding an instrument specific maximum attenuation, the filter tape moves automatically so that particles are collected in a clean part of the filter tape to avoid saturation of the filter spots.

The measurement of b_{abs} by using FAPs can be performed at different wavelengths and may have different artefacts mainly due to the interference of the filter that will depend on the type and model of instrument used.

MAAP measures b_{abs} at a single wavelength, specified as wavelength of 670 nm, although its actual wavelength is 637 nm (Müller et al., 2011). The measurement considers online artefacts related to the presence of the filter tape by simultaneously measuring the intensity of light transmitted through the aerosol-laden filter tape and scattered from the filter point at different angles, and subsequently converts this data into b_{abs}. However, as aforementioned, the MAAP is discontinued and its use in air quality monitoring sites is therefore decreasing. Petzold et al. (2013) stated that the explicit treatment of light-scattering effects caused by the aerosol and by the filter matrix in the radiative transfer scheme is expected to improve the determination of the aerosol absorption coefficient by MAAP considerably.

The Aethalometers measure the attenuation of light (b_{ATN}) passing through an aerosol-loaded filter tape at several distinct wavelengths (eg. At 370, 470, 520, 590, 660, 880, and 950 nm). The measured b_{ATN} is due to the absorption of light by BC and other absorbing particles (i.e. b_{abs}) and to measurement artefacts caused by interaction of the light with the filter fibres and the accumulation of particles on the filter. The optical absorption coefficient b_{abs} needs to be calculated from the measured b_{ATN} with consideration of these measurement artefacts.

For the determination of eBC mass concentrations, the signal at 880 nm is used because at this wavelength the b_{abs} due to other aerosol species, mostly organic aerosols, is negligible, and only BC particles absorb.

One the above-mentioned measurement artefact consists in the progressive loss of sensitivity due to the progressive accumulation of particles on the filter tape (factor loading effect; FL). Some of the available instruments correct online for FL by applying the “dual spot” method (Drinovec et al., 2015). Other instruments do no correct online for FL and offline correction is needed. Different schemes are available to correct AE data for this artefact (Drinovec et al., 2017; Segura et al., 2014; Virkkula et al., 2007; Weingartner et al., 2003).

The other artefact corrects for an increase of the measured b_{ATN} due to the scattering of light by the filter tape. Accordingly, the b_{ATN} (measured at 880 nm), once corrected for FL, either online or offline, shall be divided by the filter multiple-scattering parameter (C_0) to determine the b_{abs} at 880 nm (Eq. 2):

$$(2)\quad babs = \frac{b_{ATN}}{C_0}$$

All AE instruments convert b_{ATN} to b_{abs} using predefined and constant C_0 that depends on the filter tape used (e.g. in Savadkoohi et al. (2023)). For example, the older filter tapes (M8020 and M8050) C_0 is equal to 1.57, but for the

new filter tape (M8060) C_0 is 1.39. And in this case, the later is the recommended one and can be used on all the aethalometer models. The C_0 values are set in the instrument software and must be changed manually if the filter tape is replaced with a different one.

The multiple-scattering parameter (C_0) may differ from the one used in the software of the FAPs. Therefore, it is necessary to apply harmonization factors as such those proposed by ACTRIS (Müller and Fiebig, 2018), (see next Section on harmonization and Savadkoohi et al., 2024 for more details).

3.3.2 Determination of eBC mass concentration

The eBC mass concentrations are determined by dividing the b_{abs} by the mass absorption cross section (MAC) (Eq. 3).

$$(3)\quad eBC = \frac{babs}{MAC}$$

The MAC, measured in $m^2\ g^{-1}$, represents the absorption efficiency of BC particles and can change depending on the microphysical properties of BC. The instruments use nominal MACs for automatic determination of eBC from b_{abs}. The eBC mass concentrations are determined from MAAP by dividing the b_{abs} measured by a nominal MAC value of 6.6 $m^2\ g^{-1}$.

The most recent AEs (AE33, AE36) provide eBC mass concentration data by dividing b_{ATN} measurements at 880 nm by C_0, to obtain b_{abs}, and then by a MAC value of 7.77 $m^2\ g^{-1}$. Old AE models calculated eBC from b_{ATN} at 880 nm by using different MAC and C_0 values (see Savadkoohi et al., 2024 for more details). Wu et al. (2024) recently compared AE31 and AE33 models and concluded that the AE33/AE31 slope for equivalent BC (eBC) was 1.2, implying the need for site specific post-correction. Similarly, ACTRIS-ECAC (2016) reported a similar AE33/AE31 ratio of 1.2 for eBC mass concentration.

As aforementioned, the MAC may vary depending on the microphysical properties of BC particles and this variation should be considered for a better estimation of the eBC mass concentration (see next Section on harmonization and Savadkoohi et al., 2024, for more details).

4 HARMONIZATION OF ABSORPTION MEASUREMENTS AND eBC DETERMINATIONS

It is evident from Eqs. 2 and 3 that a robust determination of eBC mass concentration from FAPs depend on the knowledge of MAC and C_0. However, depending on the FAP considered, the default values of these parameters used by FAPs software are not always appropriate thus introducing biases in the determination of BC mass concentrations from FAPs.

4.1 Harmonization of absorption measurements

ACTRIS provides the harmonization factors necessary to convert the b_{ATN} measured with AE instruments into b_{abs}. These harmonization factors are needed because the C_0 is different from the one used in the AE software. Two parameters that depend on the type of AE and filter tape used must be considered: the default multiple-scattering enhancement parameter (C_0) and the standardized harmonization factor (H*) provided by ACTRIS (Müller and Fiebig, 2018). For AE33 and AE36 instruments, the C_0 is manually set using the instrument software and should be changed depending on the filter tape used. Recent studies have shown that the default C_0 values are not appropriate; thus, H* factors were introduced to standardize the calculation of the b_{abs}. ACTRIS proposed an H* value of 1.76 for M8060 filter tape (=2.44/1.39), while the proposed H* value for the AE33 M8020 and M8050 filter tapes was 2.21 (=3.5/1.57; Müller and Fiebig, 2018b). Currently, guidelines from the Global Atmosphere Watch

Programme suggest the use of H* = 3.5 for AE31 and AE22 (WMO/GAW, 2016; Savadkoohi et al., 2024, for more details).

The procedure used to harmonize particle light b_{abs}, is described in detail in a recent European eBC phenomenology study by Savadkoohi et al. (2023). Thus, it is crucial to have the information about the filter tape used as well as the default C_0 to apply these corrections appropriately.

It should be considered that H* can vary depending on the physical properties of particles collected on the filter tape. For example, Yus-Díez et al., (2021) showed that the C_0, and consequently the H*, increases when the single scattering albedo (SSA) of collected particles is high (>0.95). Yus-Díez et al. (2021) observed this effect, known as cross- sensitivity to scattering, at two remote/regional background sites but did not observe it at the urban site, where the SSA was low. Thus, the assumption of a constant H* is reasonably correct at the urban/traffic sites.

4.2 Harmonizing conversion of absorption into eBC mass concentration using site-specific MAC

Within the concept of harmonization, MAC is highly variable and is influenced by a range of factors including location (e.g., urban, rural, high-altitude), BC particle size, internal vs external mixing, combustion sources and instrument type. A wide range of experimental MACs have been reported in literature at different regions and seasons (Ciupek et al., 2021; Grange et al., 2020; Mbengue et al., 2021; Srivastava et al., 2022; Zanatta et al., 2016). The variation in experimental MAC values complicates the determination of precise eBC mass concentrations (Eq. 3) and, consequently, their accurate representation in air quality models. As already indicated in literature, employing the nominal MAC (i.e. default MAC set in the software instrument) results in potentially misleading eBC estimates (Savadkoohi et al., 2024, 2023). This underscores the importance of implementing harmonized methods, such as ACTRIS procedures, to ensure consistency and enable meaningful comparisons. Savadkoohi et al. (2024), in the framework of RI-URBANS, performed an in-depth analysis of how different MACs affect the conversion of b_{abs} into mass concentrations.

Site-dependent MAC values can be estimated through simultaneous measurements of b_{abs} from FAPs and EC mass concentrations from thermo-optical methods using the reference EUSAAR-2 method (Cavalli and Putaud, 2010; Karanasiou et al., 2020, 2015) (Eq. 4).

$$(4)\quad MAC = \frac{b_{abs}}{EC}$$

From Eqs. 3 and 4 it results that eBC mass concentration is only identical with EC only if the MAC value assumed for calculating eBC from b_{abs} is equal to the true MAC of the light absorbing aerosol under consideration. Once the site-dependent MAC is obtained from Eq. 4, it can be used in Eq. 3 for estimating BC mass concentration at the measuring site.

In Section 6, "*PAN-EUROPEAN OVERVIEW OF eBC*" we present the spatial and seasonal variability of MAC across Europe. We demonstrate the importance of determining site-specific MAC for the most reliable on-line eBC measurements of light absorbing particle mass concentrations, as shown by Savadkoohi et al. (2024).

Wherever simultaneous b_{abs} and EC measurements are available, conversion of b_{abs} data into EC mass concentrations measured using the CEN standard EN16909 should follow a similar protocol as for assessing the equivalence of automatic PM measurement methods to the PM gravimetric measurements described in the CEN standard EN12341. Such a protocol is described in the standard UNE-EN 16450:2017, which recommends 80 pairs of measurements, collected in a summer and a winter campaign. It can be recommended to review the validity of the equivalence at least every 2 years if there has not been any important change in the equipment in between.

However, here we do not have the reference eBC method but the PM2.5-EC CEN standard to compare, but a similar exercise is recommended.

4.3 FAPs Measurement uncertainties

The reported uncertainty for the b_{abs} values measured with a MAAP at 637 nm is 15%, as reported by Zanatta et al. (2016) and Müller et al. (2011), while Petzold and Schönlinner (2004) have reported uncertainties of 12% for b_{abs} at 637 nm. Additionally, Valentini et al. (2021) and Yus-Díez et al. (2021) and references herein, reported a possible overestimation of the b_{abs} from MAAP compared to other non-reference techniques for measuring b_{abs}. Regarding the AE33, uncertainties of around 15 % and 25% have been reported for b_{abs} and eBC, respectively (Rigler et al., 2020). Considering this, the additional aforementioned uncertainties in the measurements of b_{abs} can be minimized by continuously correcting the calculated eBC with simultaneous EC measurements performed according to the CEN standard EN16909:2017. The deviation in EC average concentrations between offline analyses according to the EN 16909:2017 standard and Semi-Continuous analyses was quantified at 18% (Karanasiou et al., 2020). Furthermore, a laboratory-to-laboratory variability of 10% in EC data has been reported by Rigler et al. (2020). This is associated with uncertainties related to the OC-EC split point, influenced by aerosol type and chemical composition and charring of organic material in thermal optical methods (Karanasiou et al., 2020; Rigler et al., 2020). Earlier studies have indicated a range of uncertainties in EC determination, spanning from 2 to 7%, in accordance with the EUSAAR-2 protocol in Europe (Cavalli and Putaud, 2010; Karanasiou et al., 2015).

The comparability of eBC mass concentrations reported in literature is partially affected by instrument-to-instrument variability. For example, Müller et al. (2011) reported a unit-to-unit variability of <5% for MAAP instruments while noting a variability of up to 30% for older AE models, such as the AE31. This large variation was primarily associated with sample flow, spot size, and the inadequacy of current correction functions. As previously mentioned, AE31 data needs to be corrected off-line for FL effects, thus contributing to the higher noise inherent in AE31 data compared to MAAP data. For example, Asmi et al. (2021) reported a difference of about 7% between MAAP and AE31 data with a low correlation coefficient (R^2 = 0.65); in contrast, the correlation between MAAP and AE33 instruments was much higher (R^2 = 0.87). Additionally, Helin et al. (2018) reported a good correlation (R^2 > 0.90) between MAAP and AE33 data, with AE33 instruments reporting slightly higher concentrations. Recently, Cuesta-Mosquera et al. (2021) reported a relatively small unit-to-unit variability of AE33-based eBC measurements, ranging between –16% and 8% with an average deviation of around –1% for eBC. In most cases, the type of filter material employed by the instruments, the total particle load on the filter, and the flow calibration, could explain the deviations. To reduce the instrument-to-instrument variability of AE33, Cuesta-Mosquera et al. (2021) recommended the use of the most recent version of filter tape (M8060) while avoiding the use of older filter tapes. Furthermore, they highlighted the importance of reporting not only the filter tape used but also the corresponding C_0 set by the internal AE settings. Due to its high accuracy and low uncertainty (12%; Petzold et al., 2005), the MAAP is considered to be the ideal reference instrument for the calculation of b_{abs}. However, we note that due to discontinuation of MAAP production, this will be not viable in the future.

5 DATA MANAGEMENT

According to EU legislation, the member states are obliged to submit the data to the European Air Quality Portal (EAQP) run by the European Environmental Agency (EEA). However, some guidance on how to do the data

management locally within the AQMNs is needed, and will be provided by EEA. Also, it is needed to clarify what will be the situation for the measurements at supersites within the NAQD? Do the member states need to send the data to EAQP from the EEA as it is the case for other air pollutants? Probably the later will be the AQ option. If this is the case, it is recommended to the EAQP to follow the data management and templates from EBAS protocols for eBC, and keep the information of the MAC values obtained to determine eBC concentrations.

In the framework of the RI-URBANS project, observational data of eBC mass concentration were compiled in WP1 (Novel air quality metrics and advanced source apportionment service tools for particulate matter and nanoparticle) from existing air quality monitoring supersites, not available at the EBAS databases (https://ebas-data.nilu.no/). These data have since been (or are being) submitted centrally to EBAS by RI-URBANS partners and not by the data owners unless they already have been submitted to other programs. The EBAS database, a major archive for data on atmospheric constituents worldwide, hosting data of different research programs and infrastructures such as the European Monitoring and Evaluation Programme (EMEP) or the WMO-GAW programme, among others. EBAS has defined, in collaboration with EUSAAR (EUSAAR - European Supersites for Atmospheric Aerosol Research) and the EU Infrastructure ACTRIS, common standard operating protocols and data reporting procedures for observations of atmospheric aerosol properties. These protocols and procedures have been adopted by the WMO-GAW program. EBAS Level 2 quality assured/quality checked (QA/QC) data including physical variables were processed following the ACTRIS recommendations for the reporting of eBC measurements.

Datasets shall include station metadata, including station type, altitude, height, and coordinates, the FAPs used, the measurement method, and any relevant operational settings (e.g., filter tape, inlet, flow rate, and reference MAC). Detailed information on methods and sampling durations should also be included in the metadata associated with the data files. However, some of the datasets directly provided by partners showed certain quality issues: certain pieces of information were missing and data had been processed in different ways and were of uneven quality levels. For this reason, data have been processed and harmonized following ACTRIS recommendations. These data were averaged hourly (see details in Savadkoohi et al., 2023). All datasets collected were presented in the open access secondary repository in ZENODO (Savadkoohi & Pandolfi, 2023; https://doi.org/10.5281/zenodo.798220). Each dataset contains metadata on the measurement site, instrument, and technical operation details. It includes b_{abs} measurements and hourly averaged eBC concentrations calculated using the nominal MAC of each instrument.

Datasets directly provided by data originators were submitted to EBAS as level 2 following the EBAS Nasa-Ames level 2 files using the template and instructions found in https://ebas-submit.nilu.no/templates/Filter-Absorption-Photometer/lev2. These datasets present b_{abs} aggregated to hourly averages. eBC mass concentrations can be calculated from the b_{abs} measurements, by using an agreed MAC, and will be made available as a level 3 product in EBAS.

In general, data management issues related to FAPs can arise in several levels, particularly regarding data quality and quality assurance and implementing measures to ensure the quality of the data and consistency. ACTRIS provides standardized measurement protocols and data processing across different instruments and sites in order to maintain consistency in data quality and enable meaningful comparisons (https://www.actris-ecac.eu/particle-light-absorption.html). Here are some potential issues and considerations, as well as suggestions for preparing data such as eBC, and b_{abs}:

- Calibration and maintenance: FAPs must be regularly calibrated and maintained to ensure accurate measurements. Any deviations can lead to data quality issues.

- Filter effects: The condition of the filters used in FAPs, such as loading and the presence of water, can affect data quality. Filters should be checked regularly, and take measures if needed (i.e. remove water, irregular shape of the loads, ...).
- Instrument configuration: Different instruments may have varying configurations, including settings for the C_0 factor. Inconsistent configurations can lead to data discrepancies.
- Data gaps and outliers: Missing data points and outliers can occur due to instrument malfunctions or other issues. These should be identified and managed carefully, ensuring that the data meets quality control standards before further analysis.
- Metadata: Comprehensive metadata (including site information, instrument type, settings, and operational details) must be recorded and managed effectively for data interpretation and comparison.
- Correct for multiple scattering: Apply a suitable C_0 factor to correct for multiple scattering in the data, which can vary depending on the instrument and the specific context of the measurements.
- Document procedures: Maintain detailed documentation of all data processing steps and assumptions for transparency and reproducibility.

6 PAN-EUROPEAN OVERVIEW OF eBC MASS CONCENTRATIONS IN URBAN EUROPE

6.1 Introduction

One specific objective of the RI-URBANS project was to interpret and reveal the benefits of obtaining datasets from urban sites on novel air quality metrics as eBC and their source contribution to provide guidelines. In this section, we describe the analysis of compiled datasets of ambient eBC measurements, including the source contributions from solid and liquid fuels.

In the framework of RI-URBANS, Savadkoohi et al. (2023), evaluated the long-term phenomenology of eBC by compiling datasets on eBC mass concentrations from 50 European monitoring sites, covering various periods between 2006 and 2022. These 50 measurement sites include 23 UB (Urban background), 18 TR (Traffic), 7 SUB (Suburban background), and 2 RB (Regional background) sites across 29 cities in 11 European countries. Figure 1 shows the distribution of monitoring sites. Table 1 provides information about the geographic region, site, city, country, station type, coordinates, altitude, measurement height, data coverage, and type of data received (Savadkoohi et al., 2023).

Spatial and temporal variability of ambient eBC mass concentrations in UB, TR, and SUB environments across Europe were studied. Data were collected primarily in UB areas, using FAPs techniques. To standardize b_{abs} calculations, ACTRIS recommended H* were applied for different AE models. These harmonized b_{abs} were then used in the AE model for eBC source apportionment. Since few sites had co-located eBC and EC measurements, the MAC for converting b_{abs} to eBC mass concentrations from the instruments was used rather than derived in situ.

Long-term trends were studied using three different approaches. First, the Theil-Sen slope regression estimator was used to calculate monthly means from hourly measurements, providing robust, non-parametric analysis of statistical significance and slope values. Only sites with at least nine years of eBC data and 75% valid measurements were included for trend analysis. Instrument changes over nine years, such as shifts from MAAP to AE33, could influence b_{abs} measurements at some sites. The Theil-Sen method focused on inter-annual trend analysis but did not consider trend shapes or breakpoints. Thus, seasonal-trend decomposition time series (STL) analysis, based on

the 'Loess' estimator, was employed to examine trends and seasonal variations. Bootstrapped 95% confidence intervals were calculated for both STL and Theil-Sen results.

Finally, piecewise regression using the "segmented" package identified potential breakpoints that segment trends. An interactive procedure, incorporating approximate breakpoint values and bootstrap restarting, estimated segment slopes and statistical significance.

Table 1. *List of the 50 monitoring sites that have supplied eBC mass concentration datasets. The table includes detailed information such as the location of each site, the type of site (UB, Urban Background; TR, Traffic; SUB, Suburban Background; RG, Regional Background), the instrument used for measurements, and specific measurement details including altitude and measurement height. The table presents eBC mass concentration and absorption coefficient (b_{abs}) data from various countries, including Finland (FI), Sweden (SE), United Kingdom (UK), Netherlands (NL), France (FR), Spain (ES), Greece (GR), Romania (RO), Germany (DE), Switzerland (CH), and Italy (IT). The eBC mass concentration values are reported in units of μg m^{-3}. The type of data received indicates whether it is compiled as eBC mass concentration or absorption coefficient. The data is categorized as either hourly averaged (supplied by data providers) or raw data, which refers to raw data obtained directly from the instrument with original time resolution. Level 2 data refers to quality-checked hourly averaged data that has been downloaded from the EBAS database. Modified from Savadkoohi et al. (2023).*

Region	Site	City Country	Type	Acronym	Coordinates	Altitude (m.a.s.l.)	Instrument	measurement height [m]	Data received	Data source	Data coverage
Northern Europe	Mannerheimintie	Helsinki-FI	TR	HEL_TR1	60.1697, 24.939	10	MAAP	4	eBC	RI-URBAN (Hourly)	01/01/2011-12/31/2019
	Mäkelänkatu	Helsinki-FI	TR	HEL_TR2	60.196, 24.952	25	MAAP	4	eBC	RI-URBAN (Hourly)	01/30/2015-12/31/2019
	Töölöntulli	Helsinki-FI	TR	HEL_TR3	60.190, 24.916	24	MAAP	4	eBC	RI-URBAN (Hourly)	11/01/2010-30/12/2015
	Kehä I	Helsinki-FI	TR	HEL_TR4	60.241, 25.025	15	MAAP	4	eBC	RI-URBAN (Hourly)	01/01/2012-12/28/2012
	Tikkurila	Helsinki-FI	TR	HEL_TR5	60.289, 25.039	22	MAAP	4	eBC	RI-URBAN (Hourly)	Years 2014, 2016 & 2018
	Leppävaara	Helsinki-FI	TR	HEL_TR6	60.220, 24.811	13	MAAP	4	eBC	RI-URBAN (Hourly)	Years 2015 & 2017
	Kallio	Helsinki-FI	UB	HEL_UB	60.1872, 24.950	18	MAAP	4	eBC	RI-URBAN (Hourly)	01/04/2012-12/31/2019
	Rekola	Helsinki-FI	SUB	HEL_SUB1	60.331, 25.075	29	AE33	4	7 (λ) eBC	RI-URBAN (Hourly)	05/01/2017-31/05/2017
	Itä-Hakkila	Helsinki-FI	SUB	HEL_SUB2	60.291, 25.112	41	AE33	4	7 (λ) eBC	RI-URBAN (Hourly)	03/01/2018-23/10/2018
	Pirkkola	Helsinki-FI	SUB	HEL_SUB3	60.234, 24.922	27	AE33	4	7 (λ) eBC	RI-URBAN (Hourly)	31/12/2018-31/12/2019
	SMEAR II	Hyytiälä, FI	RB	SMR_RB	61.847, 24.295	181	AE33	4	7 (λ) eBC & 7 (λ) babs	RI-URBAN (Hourly)	15/03/2018-31/12/2021
						181	AE31	4	7 (λ) eBC & 7 (λ) babs	RI-URBAN (Hourly)	31/05/2006-17/11/2017
						181	MAAP	4	eBC	RI-URBAN (Hourly)	18/06/2013-09/05/2021

	Hornsgatan 108	Stockholm -SE	TR	STH_TR	59.3171, 18.048	25	AE33	4	7 (λ) eBC	RI-URBAN (Hourly)	14/10/2014-31/12/2019
						25	MAAP	4	eBC	RI-URBAN (Hourly)	04/11/2015-05/12/2016
	Torkel Knutssonsgatan	Stockholm -SE	UB	STH_UB	59.316, 18.057	48	AE33	24	7 (λ) eBC	RI-URBAN (Hourly)	10/14/2014-12/31/2019
						48	MAAP	24	eBC	RI-URBAN (Hourly)	10/02/2014-11/3/2015
North-Western Europe	BAQS	Birmingham-UK	UB	BIR_UB	52.455, -1.928	143	AE33	3	7 (λ) eBC	RI-URBAN (Hourly)	03/19/2019-2/23/2022
	North Kensington	London-UK	UB	LND_UB	51.521, -0.213	27	AE22	2.8	2 (λ) eBC	RI-URBAN (Hourly)	01/01/2009-11/07/2019
						27	AE33	2.8	7 (λ) eBC	RI-URBAN (Hourly)	01/01/2020-01/01/2022
	Marylebone Road	London-UK	TR	LND_TR	51.522, -0.1546	35	AE22	3	2 (λ) eBC	RI-URBAN (Hourly)	16/03/2009-31/12/2019
						35	AE33	3	7 (λ) eBC	RI-URBAN (Hourly)	01/24/2020-01/01/2022
Western Europe	Winkelhorst	Enschede-NL	UB	NLD_UB1	52.234, 6.919	38	MAAP	3	eBC	RI-URBAN (Hourly)	04/29/2015-12/31/2021
	Nijensteinheerd	Groningen-NL	UB	NLD_UB2	53.246, 53.246	-1	MAAP	3	eBC	RI-URBAN (Hourly)	05/04/2015-12/31/2021
	Jamboreepad	Heerlen-NL	UB	NLD_UB3	50.900, 5.986	98	MAAP	3	eBC	RI-URBAN (Hourly)	04/09/2015-12/31/2021
	Ruyterstraat	Nijmegen-NL	UB	NLD_UB4	51.838, 5.856	28	MAAP	3	eBC	RI-URBAN (Hourly)	04/30/2015-12/31/2021
	Europalaan	Veldhoven-NL	UB	NLD_UB5	51.407, 5.393	22	MAAP	3	eBC	RI-URBAN (Hourly)	05/21/2015-12/31/2021
	Noordbrabantlaan	Eindhoven - NL	TR	NLD_TR1	51.444, 5.444	18	MAAP	3	eBC	RI-URBAN (Hourly)	28/04/2015-31/12/2021
	Graafseweg	Nijmegen-NL	TR	NLD_TR2	51.841, 5.857	28	MAAP	3	eBC	RI-URBAN (Hourly)	26/05/2015-31/12/2021
	NL01487 (RPW)	Rotterdam - NL	TR	NLD_TR3	51.891, 4.481	2	MAAP	4	eBC	RI-URBAN (Hourly)	01/01/2010-31/12/2021
	NL01488 (RZW)	Rotterdam-NL	UB	NLD_UB6	51.894, 4.4876	0	MAAP	4	eBC	RI-URBAN (Hourly)	01/01/2010-12/31/2021
	NL01492 (RDM)	Rotterdam - NL	TR	NLD_TR4	51.914, 4.48	-1	MAAP	4	eBC	RI-URBAN (Hourly)	01/07/2007-31/12/2021
	Paris-13	Paris-FR	UB	PAR_UB	48.828, 2.359	57	AE33	2.3	7 (λ) eBC	RI-URBAN (Hourly)	01/01/2016-12/31/2019
	Haussmann	Paris-FR	TR	PAR_TR	48.874, 2.330	42	AE33	3.8	7 (λ) eBC	RI-URBAN (Hourly)	01/01/2016-12/29/2019
	ATOLL	Lille-FR	SUB	LIL_SUB	50.611, 3.1403	70	AE33	20	7 (λ) eBC	RI-URBAN Raw data	01/01/2017-31/12/2019
	SIRTA	Paris-FR	SUB	PAR_SUB	48.7086, 2.1588	162	AE33	15	7 (λ) eBC	RI-URBAN (Hourly)	01/01/2014-30/12/2020

South-western Europe	Longchamp	Marseille-FR	UB	MAR_UB	43.305, 5.394	73	AE33	3	7 (λ) eBC	RI-URBAN (Hourly)	01/01/2017-12/31/2019
	Palau Reial	Barcelona-ES	UB	BCN_UB	41.387, 2.115	80	AE33	4	7 (λ) eBC & 7 babs	RI-URBAN (Hourly)	04/03/2015-9/20/2020
						64	MAAP	4	eBC	RI-URBAN (Hourly)	01/13/2009-3/31/2021
	UGR	Granada-ES	UB	GRA_UB	37.18, -3.58	680	AE33	15	7 (λ) eBC	RI-URBAN (Hourly)	01/01/2014-12/31/2019
						680	MAAP	15	eBC	RI-URBAN (Hourly)	01/01/2006-31/12/2020
	CIEMAT	Madrid-ES	UB	MAD_UB	40.456, -3.725	669	AE33	4	7 (λ) eBC	RI-URBAN (Hourly)	14/01/2013-31/12/2019
	Burjassot	Valencia-ES	UB	VLC_UB	39.51, -0.42	40	AE31	15	7 (λ) eBC & 7 babs	RI-URBAN (Hourly)	01/09/2017-12/7/2020
South-Eastern Europe	Thissio	Athens-GR	UB	ATH_UB	37.973, 23.718	105	AE33	4	7 (λ) eBC & 7 ATN	RI-URBAN (Hourly)	01/01/2017-12/31/2019
	Demokritos	Athens-GR	SUB	ATH_SUB	37.99, 23.82	270	AE33	6	7 (λ) babs	RI-URBAN (Hourly)	11/01/2017-31/12/2019
Eastern Europe	INO	Bucharest-RO	SUB	BU_SUB	44.348, 26.029	93	AE33	15	7 (λ) eBC	RI-URBAN Raw data	27/02/2014-11/01/2022
Central Europe	Winckelmannstrasse	Dresden-DE	UB	DDW_UB	51.036, 13.730	120	MAAP	3.5	eBC	RI-URBAN (Hourly)	01/01/2017-12/31/2019
	Nord	Dresden-DE	TR	DDN_TR	51.087, 13.7630	112	MAAP	4	eBC	RI-URBAN (Hourly)	01/01/2017-31/12/2019
	TROPOS	Leipzig-DE	UB	LEJ_UB	51.352, 12.434	113	MAAP	4	babs_670 nm	EBAS Level 2	01/01/2009-12/31/2020
	Mitte	Leipzig-DE	TR	LEJ_TR1	51.344, 12.377	111	MAAP	4	babs_670 nm	EBAS Level 2	04/01/2017-26/12/2019
	Eisenbahnstrasse	Leipzig-DE	TR	LEJ_TR2	51.345, 12.406	120	MAAP	4	babs_670 nm	EBAS Level 2	17/01/2009-31/12/2020
	Bollwerk	Bern-CH	UB/TR	BER_UB	46.951, 7.440	536	AE33	4	7 (λ) babs	RI-URBAN (Hourly)	01/01/2015-12/31/2021
	Università	Lugano-CH	UB	LUG_UB	46.011, 8.9572	287	AE33 & MAAP	3	babs 880nm	RI-URBAN (Hourly)	11/03/2021-12/31/2021
						287		3	babs 670 nm	RI-URBAN (Hourly)	11/03/2021-12/31/2021
	Kaserne	Zurich-CH	UB	ZUR_UB	47.3775, 8.5305	409	AE33	3	7 (λ) babs	RI-URBAN (Hourly)	01/01/2012-12/31/2021
	Pascal	Milan-IT	UB	MLN_UB	45.464, 9.188	118	AE33	2.5	7 (λ) eBC & 7 babs	RI-URBAN (Hourly)	06/08/2018-11/04/2019
						118	MAAP	2.5	eBC	RI-URBAN (Hourly)	06/02/2013-21/11/2021
	Senato	Milan-IT	TR	MLN_TR1	45.464, 9.188	121	AE33	2.5	7 (λ) eBC	RI-URBAN (Hourly)	12/06/2019-22/11/2021

	Marche	Milan-IT	TR	MLN_TR 2	45.464, 9.188	129	AE33	2.5	7 (λ) eBC	RI-URBAN (Hourly)	12/06/2019-22/11/2021
	Ispra	IPR_IT	RB	IPR_RB	45.8, 8.633	209	EBAS MAAP	9	babs_670 nm	EBAS Level 2	16/09/2008-31/12/2020

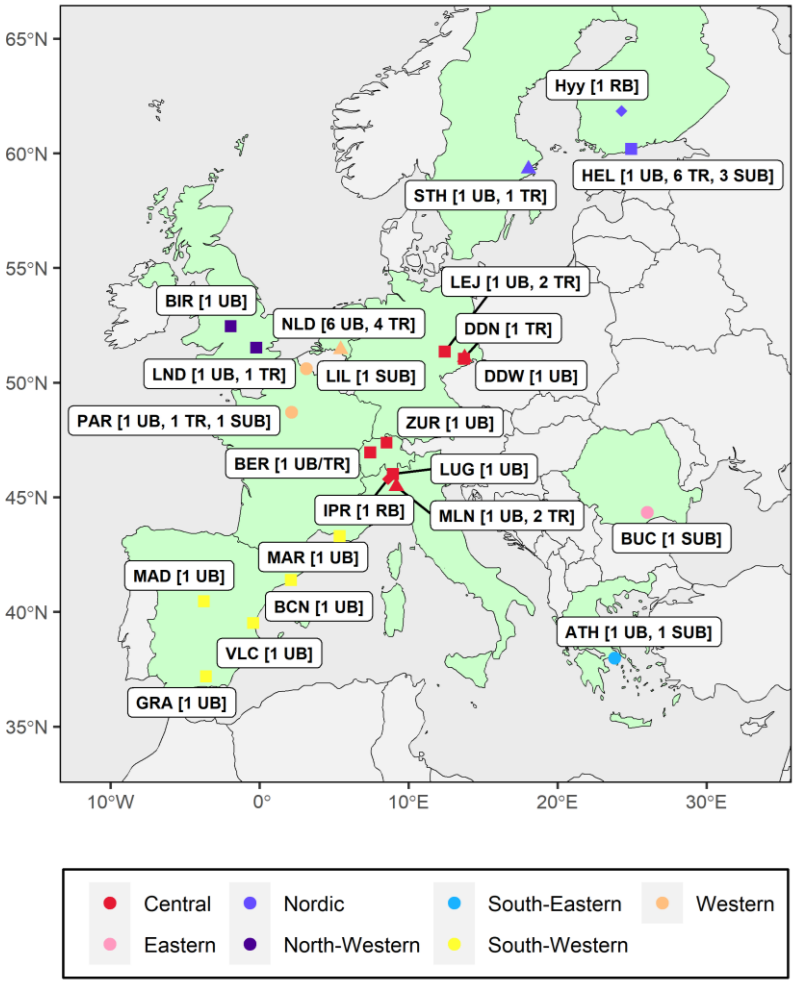

Figure 1. *Distribution of the monitoring sites with eBC data. UB: urban background; SUB: suburban background; TR: traffic; RB: regional background. Modified from Savadkoohi et al. (2023).*

6.2 eBC spatial variability in urban Europe

The harmonized dataset indicated a significant decreasing trend in eBC mass concentrations, generally ranked as TR > UB > SUB > RB. However, there were exceptions, such as high eBC values observed at a rural site in the Po Valley (Northern Italy), known for its PM pollution. Average eBC mass concentrations varied from 3.4 μg m^{-3} at a traffic site in Milano, Italy (MLN_TR2), to 0.17 μg m^{-3} at a regional background site in Hyytiälä, Finland (at SMEAR_RB), based on data from 2017 to 2019. A notable north–south gradient in eBC mass concentrations, in line with other pollutants like NO_2 or $PM_{2.5}$, reflected regional differences in emissions. Seasonal variability in eBC mass concentrations was evident, with the highest levels observed during winter at the above Milan traffic site (MLN_TR2) (5.2 ± 2.8 μg m^{-3}) and the lowest in summer at the Finnish regional background site (SMEAR_R) (0.1 ±

0.1 µg m^{-3}). Figure 2 shows the variability of eBC mass concentrations across various regions, based on hourly averaged data from the corresponding stations during the study period (2017–2019).

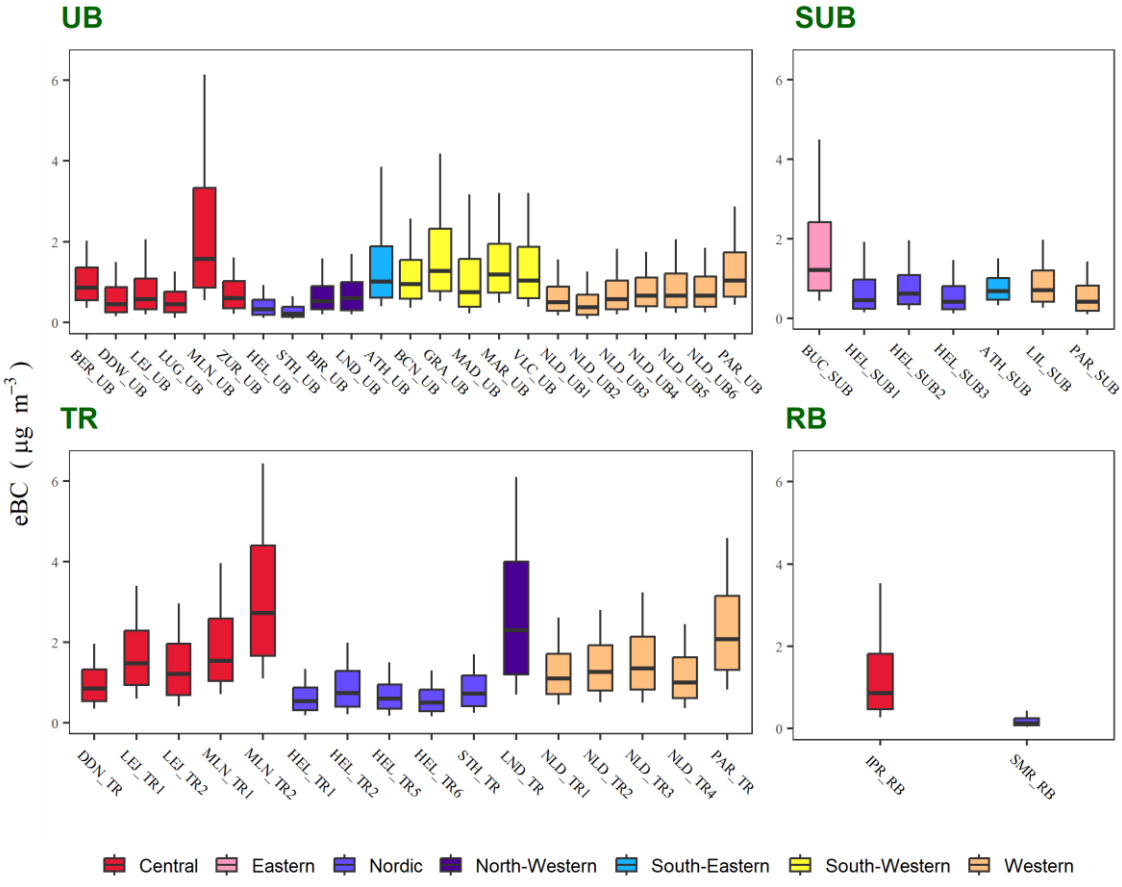

Figure 2. *Variability of hourly averaged eBC mass concentrations at 50 sites between 2017 and 2019 categorized by the type of site and region. Modified from Savadkoohi et al. (2023).*

The aethalometers, measuring absorption at several wavelengths, provide information about the of eBC originating from liquid fuel combustion (e.g., vehicular exhaust emissions; eBC_{LF}) and solid fuel combustion (primarily from residential and commercial wood and coal burning; eBC_{SF}) across different urban, traffic, and regional background environments. These contributions are commonly estimated by applying the so-called Aethalometer model (AE model). A detailed review and recommendations on eBC source distribution are presented in the specific sections of ST11 of RI-URBANS at: https://riurbans.eu/project/#service-tools. Preliminary results on eBC source apportionment by applying the AE model are presented in Savadkoohi et al. (2023) showing eBC_{LF} (mainly attributed to road traffic) is the primary contributor to urban eBC (up to 88%), with an increasing contribution from northern to central, western, and south-western Europe. However, eBC_{SF}, mainly related to biomass and coal combustion, plays a significant role in certain cities (26−39% in Bucharest, Athens and Helsinki).

6.3 Trend analysis of eBC

Figure 4 represents the estimated obtained inter-annual trends of the eBC mass concentrations for the selected sites. At all sites, a consistent statistically significant decreasing trend was detected during the observation periods. Decreasing eBC mass concentration trends varied from −1.6% to −8.4% annually (Savadkoohi et al., 2023). The most significant absolute trends in eBC mass concentrations occurred at TR sites, ranging from −0.09 µg m^{-3} yr−1 to −0.9

µg m^{-3} yr−1. At UB and RB stations, trends ranged from −0.02 to −0.1 µg m^{-3} yr−1 and −0.01 to −0.07 µg m^{-3} yr−1, respectively. Savadkoohi et al. (2023) evaluated the long-term evolution of the estimated concentrations of eBC_{LF} and eBC_{SF}. A decreasing trend was revealed for eBC_{LF} over the last decade, while eBC_{SF} remained relatively constant or even increased slightly in some sites. The decrease in eBC is therefore linked to the decrease in eBC_{LF}, reflecting the high effectiveness of European policies on air quality and emissions at European, national, regional and local level, in particular the implementation of diesel particulate filters (DPF) from 2011 on EURO5 vehicles.

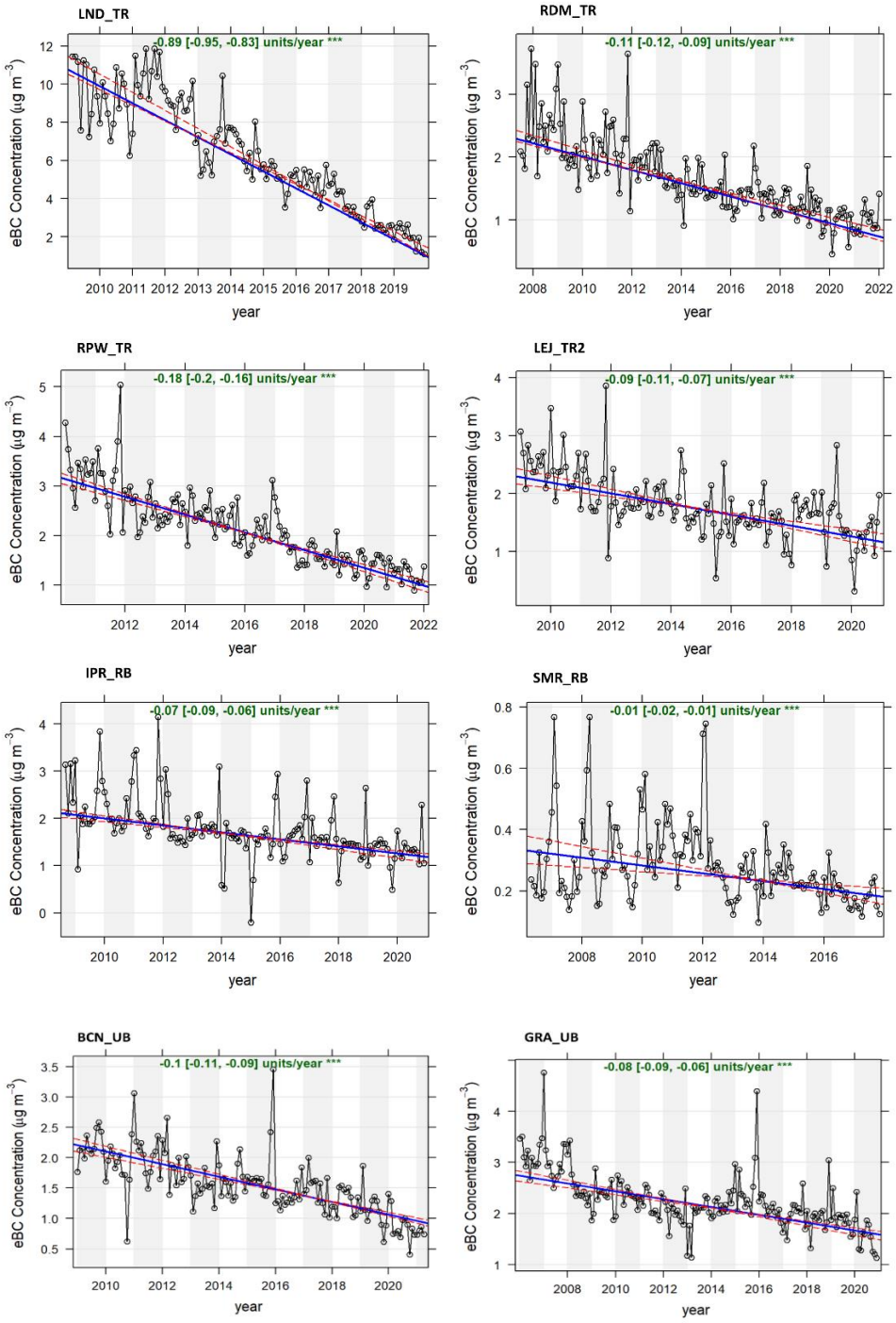

Figure 3. *eBC mass concentration trends for selected TR and RB sites. The slope of the trends are given in % yr-1 (in green). The statistically significant trends of each site are represented by *** for p < 0.001, ** for p < 0.01, * for p < 0.05, + for p < 0.1, and ns for not significant. Modified from Savadkoohi et al. (2023).*

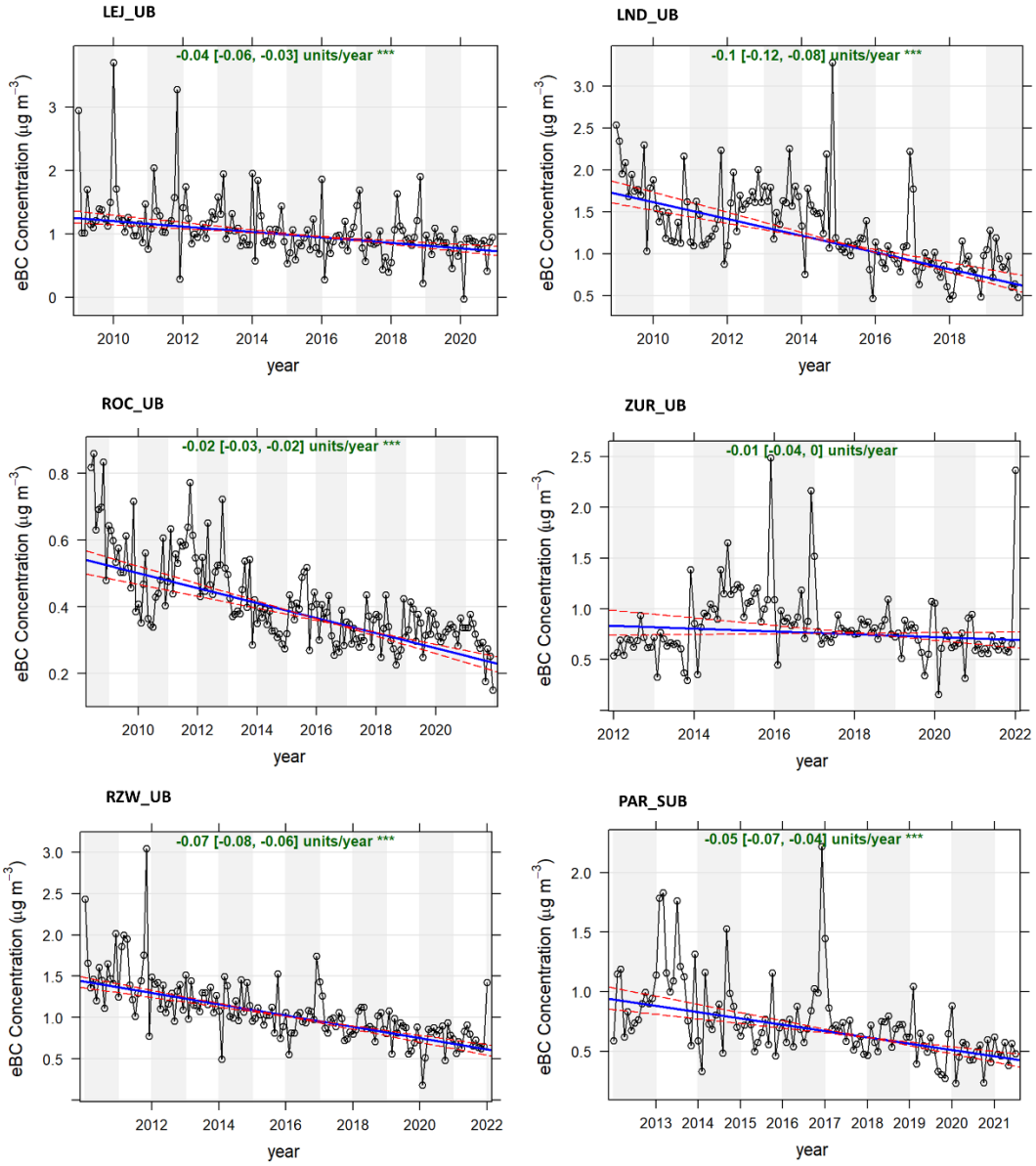

Figure 3. *Continued. eBC mass concentration trends for selected UB and SUB sites. The slope of the trends are given in % yr-1. The statistically significant trends of each site are represented by *** for p < 0.001, ** for p < 0.01, * for p < 0.05, + for p < 0.1, and ns for not significant. Modified from Savadkoohi et al. (2023).*

6.4 Determination of site-specific MAC

Out of the 50 European monitoring sites supplying FAPs data to the RI-URBANS project (Savadkoohi et al., 2023), 22 sites (21 in Europe and 1 in the US) also reported measurements of EC mass concentrations. These 22 measurement sites were collected from 18 cities, including 13 urban (UB), 4 traffic (TR), 2 sub-urbans (SUB), and 3 regional background (RB) sites. Figure 4 shows the distribution of the sites. The FAPs used at the 22 sites included the AE33 model at 9 sites and the MAAP at 10 sites. Additionally, three sites (London_UB, London_TR, and Rochester_UB) provided data using the AE22 or AE21 models. EC mass concentrations were measured using thermal-optical organic/elemental carbon (OC-EC) Sunset analysers, either offline or online.

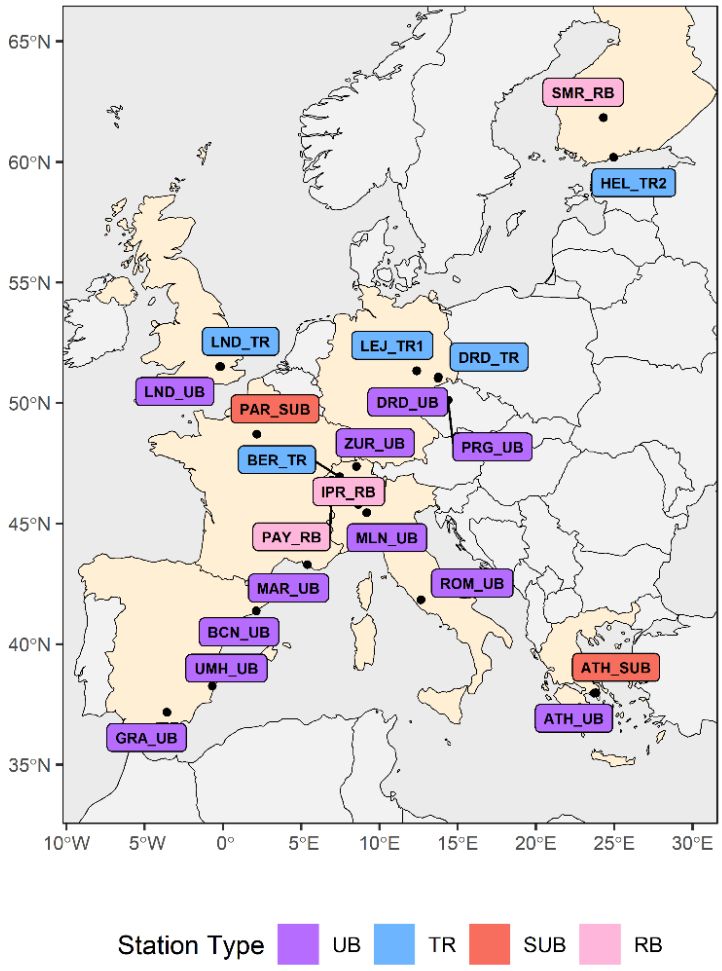

Figure 4. *Locations and types of monitoring sites with equivalent black carbon (eBC) and elemental carbon (EC) mass concentration data. Modified from Savadkoohi et al. (2024).*

Following Eq. 4, the spatiotemporal variability of the MAC was studied using simultaneous measurements of EC and b_{abs} at 22 sites. Detailed description of the methodology and data processing can be found in the study by Savadkoohi et al. (2024). Briefly, the experimental MAC values at each site were calculated from Eq. 4 using the b_{abs} from MAAP at 637 nm and the b_{abs} from AE33, AE21, and AE22 instruments at 880 nm.

6.5 Spatial variability and seasonality of experimental MAC

The resulting experimental MAC values showed a strong spatial-temporal variability. The median MAC values obtained were 7.8 ± 3.4 $m^2\ g^{-1}$ at 880 nm from 12 AEs and 10.6 ± 4.7 $m^2\ g^{-1}$ at 637 nm from 10 MAAPs, which align closely with the recommended ACTRIS value of 10.0 $m^2\ g^{-1}$ at 637 nm (i.e., 7.2 $m^2\ g^{-1}$ at 880 nm) based on prior study by Zanatta et al. (2016).

The difference between the nominal MAC employed in FAPs and the median MAC values reported here was particularly pronounced for MAAP, which uses a MAC of 6.6 $m^2\ g^{-1}$ at 637 nm for reporting eBC concentrations. In contrast, the nominal MAC value at 880 nm for AE33 instruments (7.77 $m^2\ g^{-1}$) closely aligned the median MAC reported in this study (7.8 $m^2\ g^{-1}$). Nonetheless, the primary source of uncertainty in AE33-reported nominal eBC values stems from using a C_0 value of 1.39 in the AE33 software. This value is roughly 45% lower than the 2.44 value selected for harmonizing b_{abs} measurements from AE33 instruments, as observed in prior research (Müller and Fiebig, 2018).

A comparison between eBC concentrations obtained using nominal MAC and experimental MAC values consistently showed eBC using nominal MAC overestimated eBC from experimental MAC by 40% to 80%. Given the strong spatial variability of experimental MAC values, local estimation of the MAC from simultaneous b_{abs} and EC measurements is the most effective approach to reduce BC uncertainty. Figure 5 shows the experimentally determined MAC for MAAPs and AEs, normalized through concurrent EC measurements by site typology.

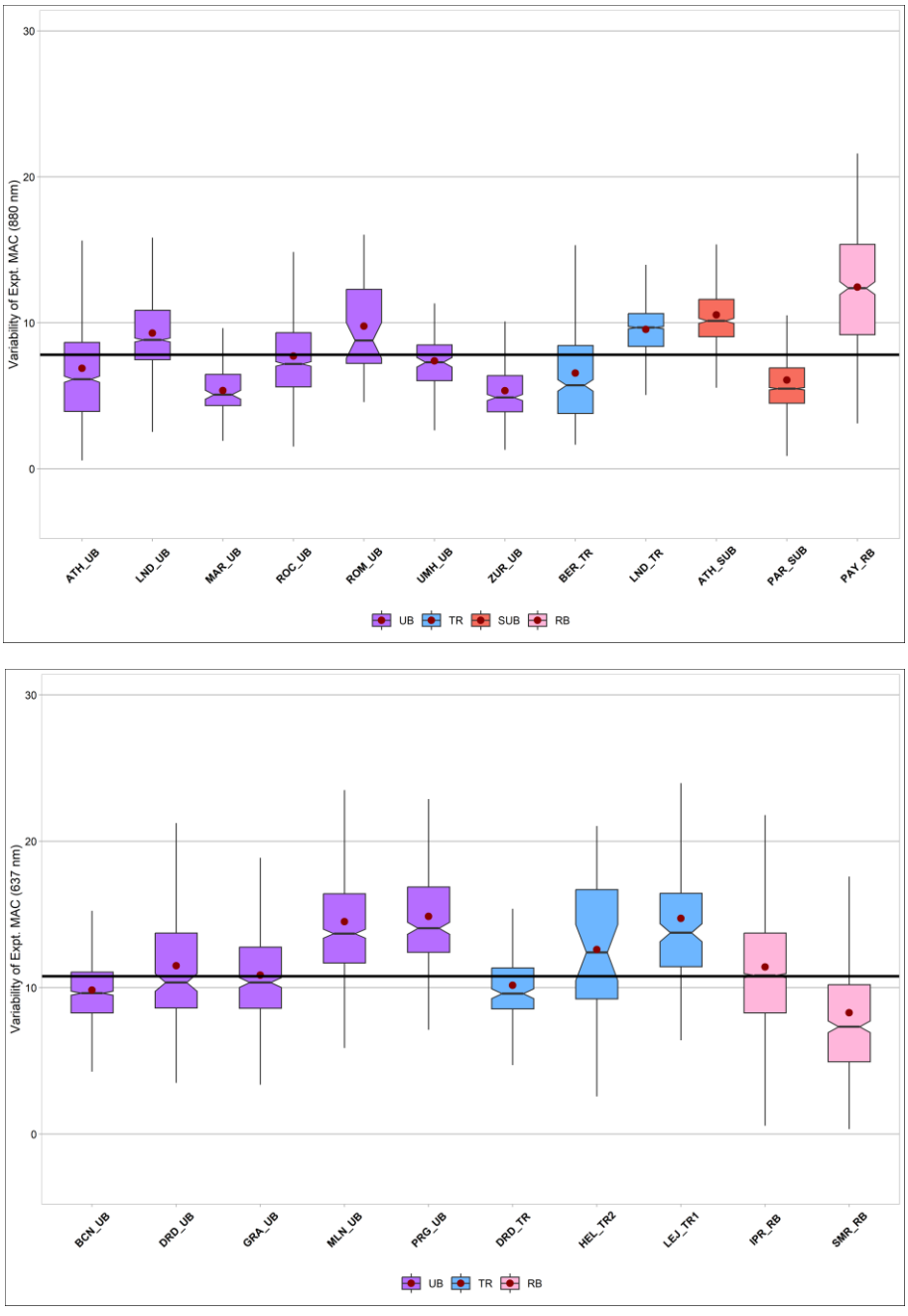

Figure 5. *Variation in experimental MAC at instrument-specific wavelengths (AEs: 880 nm), grouped by site type (urban background [UB], suburban background [SUB], traffic [TR], and regional background [RB]). The solid black line denotes the total experimental median MAC for 12 AEs at 880 nm (7.8 ± 3.4 $m^2\ g^{-1}$). Modified from Savadkoohi et al. (2024).*

Considering the temporal variability of the MAC, continuous simultaneous measurements of b_{abs} and EC are recommended which allows estimating a rolling (time-dependent) MAC as the optimal conversion factor for

estimating mass concentrations from optical measurements. This approach continuously normalizes eBC concentrations to EC concentrations, which exists as a reference method (EN 16909, 2017). Accordingly, as shown in Figure 6, the difference between eBC calculated by using the nominal MAC and the rolling MAC reached up to 70%.

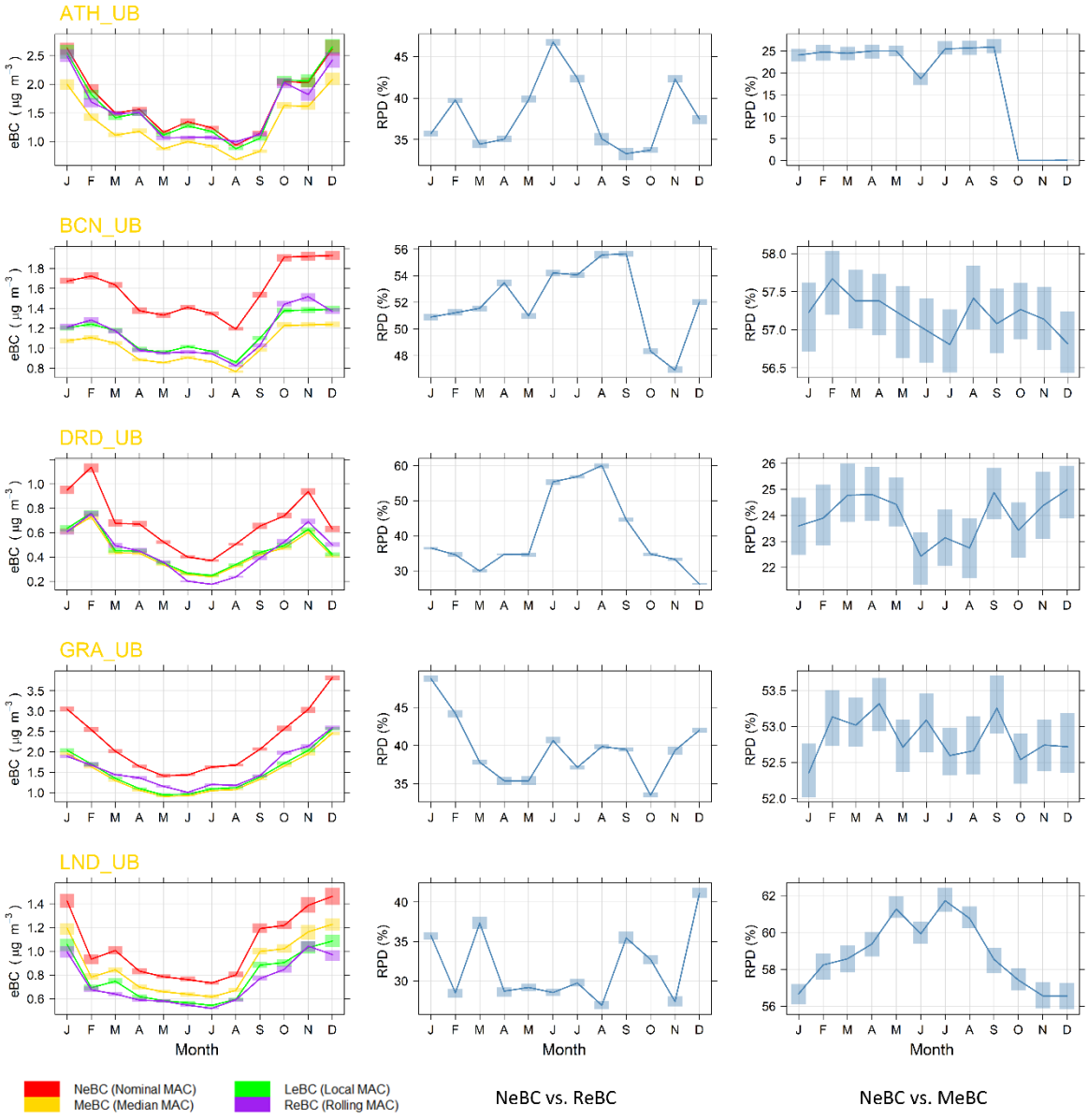

Figure 6. Monthly variations in eBC mass concentration using experimental MAC values at 880 and 637 nm. The relative percentage difference (RPD%) is computed by assessing the relative variance between the eBC using the nominal MAC (NeBC) and using rolling MAC (ReBC) and the median MAC (M_eBC). Modified from Savadkoohi et al. (2024).

Long-term continuous normalization is essential for analysing eBC trends. Using any constant MAC value (nominal, local, or median) could mislead eBC trend interpretation if there is also a trend in MAC. For example, as shown in Figure 7, at the ROCHESTER_UB site, a statistically significant decreasing trend in N_eBC concentrations was observed at a rate of -3.76% per year. The estimated experimental MAC also showed a statistically significant

declining trend of -3.76% per year. In contrast, the EC concentration demonstrated a slight, non-significant increase of 1.2% per year. However, using the rolling MAC, almost no statistically significant trend was observed for R_eBC at Rochester (0.56% per year). This indicates that the long-term trends of eBC accurately reflect the EC trends only when the rolling MAC is employed. Thus, using a constant MAC value can lead to misleading interpretations of eBC trends if the MAC itself trends over time (see Figure 8).

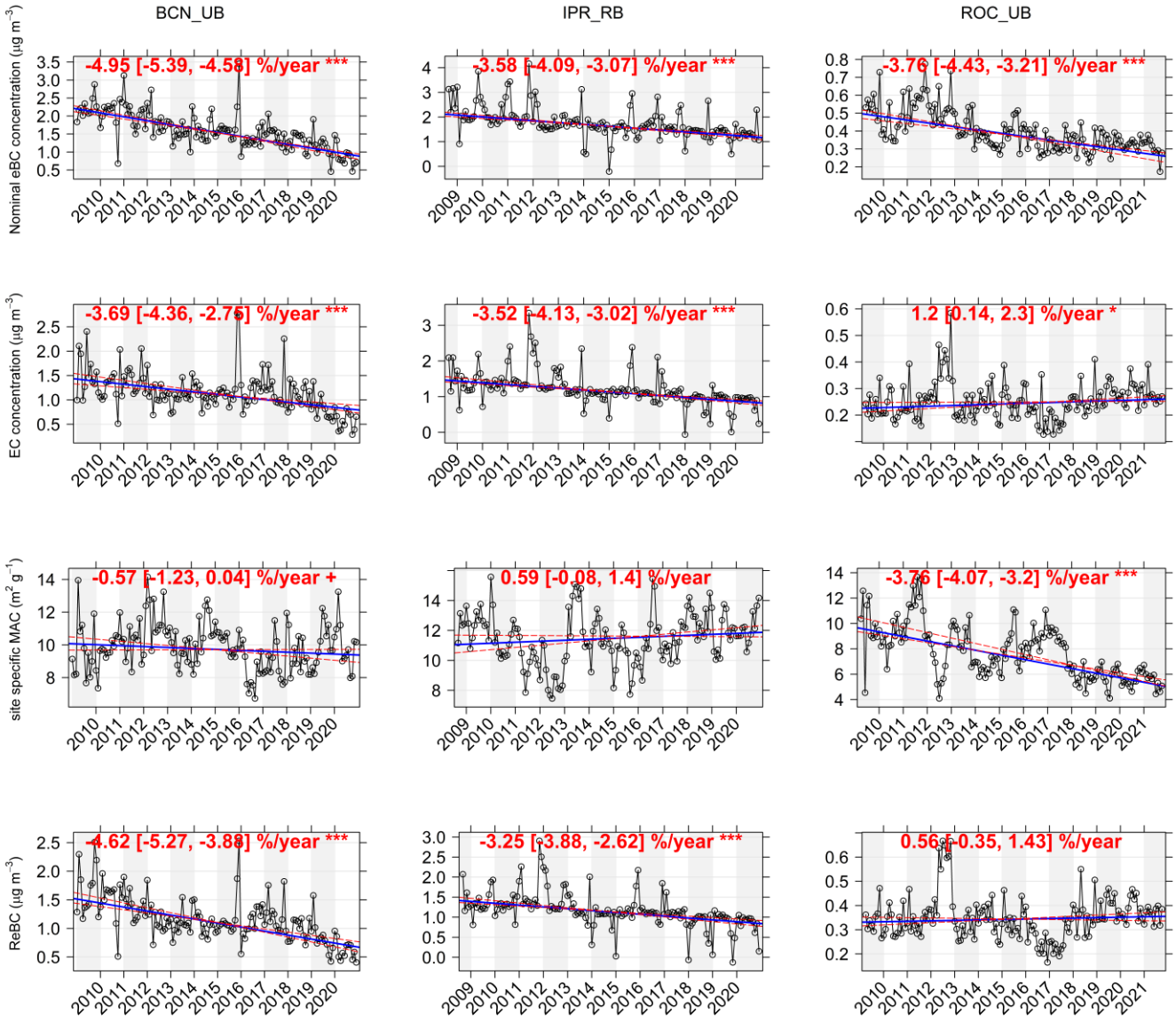

Figure 7. (a) Trends of nominal eBC mass concentrations, (b) EC mass concentration, (c) experimental site-specific MAC at 880 and 637 nm and (d) R_eBC mass concentrations (corrected by rolling MAC). The slope of the trends is given in % yr^{-1}. Trend slopes with 95% confidence interval (CI) were calculated using the Theil-Sen method with de-seasonalized data. Statistical significance is marked by "***" (p<0.001), "**" (p<0.01), "*" (p<0.05) and "+" (p<0.1). Modified from Savadkoohi et al. (2024).

7 RECOMMENDATIONS AND MAIN FINDINGS

7.1 Recommendations on measurements

Below we summarize the recommendations for the determination of BC by using FAPs.

7.1.1 Sampling system

A PM_{10} inlet should be generally used. This cut-off is harmonized with the WMO-GAW network. To measure aerosol particles the air inlet must be generally between 1.5 m and 4 m above the ground (2008/50/EC). Sampling tubes should be made of a conductive, corrosion-resistant material with a low surface roughness (e.g., stainless steel). Aerosol in-situ measurements should be done at a relative humidity lower than 40%. Performing the clean air test weekly is recommended.

7.1.2 Recommendations on determining eBC in µg m^{-3}

- Complying with the GAW and ACTRIS guidelines for instrument operation in the absence of standard for eBC measurement.
- Applying the appropriate Aethalometer harmonization factor H* values depending on the filter tape used.
- eBC is calculated from b_{abs} using an appropriate MAC. There are different options for determining the MAC value, one is using the ACTRIS recommended value, another is determining the MAC from comparison of b_{abs} and EC. Important is that there are different ways leading to eBC values that are NOT comparable across different AQMNs, when they use different approaches for determining the MAC. This is very important.
- An approach to ensure comparability across networks would be to follow CEN Technical Report TR18076:2024 and to show that the measurements of the FAP is equivalent to the reference method for EC. Such a calculated measurand would be called EC, because it is equivalent to reference EC measurements (in analogy what is done for PM2.5 and PM10).
- The "equivalence" in eBC has a historical origin, it should not be mixed up with the equivalence as stated in the Guide for the Demonstration of Equivalence (GDE) used for AQ purposes, were eBC does not fulfil the requirement because of i) how it is defined and ii) there is no reference method for eBC.
- RI-URBANS recommends applying site-specific MAC, whenever feasible, instead of relying on nominal MAC values from instrument manufacturers.
- Expanding monitoring networks to include regular EC measurements to improve knowledge of site-specific MAC values for improved estimation of eBC mass concentrations.
- Continuously measuring b_{abs} and EC in order to estimate a time-dependent rolling MAC.
- If continuous long term b_{abs} and EC measurements are not possible, one year of b_{abs} and EC should be planned to estimate a median site-dependent MAC value to be applied to past and future measurements.
- Estimating a site-dependent value should follow a protocol similar to the one described in the European standard EN 16450:2017 to assess the equivalence of automatic PM measurement methods to the PM gravimetric method described in the European standard EN12341:2023.
- When EC observations are unavailable, we recommend using the median MAC value of 10.6 $m^2\ g^{-1}$ determined in RI-URBANS for b_{abs} data from MAAP at 637 nm.
- It is important to note that EC measurements performed with the EC standard (EN16909:2016), EC concentrations are reported in ambient conditions, not in standard volume ones. Thus, when applying the when local MAC by comparison b_{abs} with EC, the resulting eBC concentrations are given also in ambient conditions, as the AQ directives require for PM pollutants.

7.2 Recommendations on data management

- Collecting information on various parameters for AE instruments including filter tape type and characteristics (such as multiple-scattering parameter and leakage factor set in the instrument), inlet size-cut and length, and measurement conditions (temperature, pressure, and humidity) (Savadkoohi et al., 2023).
- Following the EBAS protocols for data reporting and data management established by EBAS in collaboration with ACTRIS. In this context, EBAS defined 3 data levels and corresponding data file formats: Level 0, Level 1, and Level 2. FAPs data, metadata and flags can be reported for each Level as indicated in EBAS Data Centre (https://ebas-submit.nilu.no/templates/Filter-Absorption-Photometer). Level 2 data contains hourly averages and concentration stated for standard temperature and pressure conditions (273.15 K; 1013.25 hPa). Detailed measurement guidelines and the standard operating procedures (SOPs) relevant for observations reported to EBAS can be found in https://ebas-submit.nilu.no/SOPs.
- Please also note that ACTRIS is reporting concentrations according to standard conditions. However, EBAS data products can also be downloaded according to ambient air conditions, when needed.

7.3 Main findings for eBC observations at urban sites across Europe

- There is a notable lack of monitoring BC at traffic sites in Southern Europe.
- Urban eBC mass concentrations are higher in southern and eastern Europe compared to Northern Europe, reflecting patterns seen with other air pollutants.
- A gradient of eBC concentrations from traffic > urban background > regional background sites emphasize traffic as the major source of eBC.
- Source apportionment of eBC into eBC_{SF} (solid fuels, primarily domestic biomass or coal combustion) and eBC_{LF} (diesel vehicles, liquid fuel fired boilers) indicates road traffic is the primary contributor to urban eBC (up to 88%). However, eBC from biomass and coal combustion plays a significant role in certain cities (26–39% in Bucharest, Athens and Helsinki).
- Trend analyses revealed notable annual decreases in eBC mass concentrations, ranging from −1.6% to −8.4%. The most pronounced trends were observed at traffic sites (−0.09 to −0.9 μg m^{-3} yr^{-1}), with smaller decreases at urban (−0.02 to −0.1 μg m^{-3} yr^{-1}) and regional (−0.01 to −0.07 μg m^{-3} yr^{-1}) background stations. eBC trends suggest a decline in road traffic emissions over the last decade, while eBC from biomass and coal combustion has remained stable or increased.

7.4 Recommendations on eBC measurements for policy making support

- Harmonization of instrumentation and measurement protocols, including the conversion of absorption coefficients to equivalent black carbon (eBC), is crucial. Discrepancies of up to 50% in eBC concentrations can arise from using the same instruments at the same site due to different measurement protocols.
- Expanding monitoring programs at urban sites to include regular EC measurements and combining EC measurements with b_{abs} data to enable a more accurate estimation of the mass concentration of light absorbing particles for air quality assessment.
- The decline in eBC concentrations reflects the effectiveness of EU policies on air quality and emissions, particularly the adoption of Diesel Particulate Filters (DPFs) in EURO5 vehicles from 2011 onwards. Continued measures to mitigate road traffic emissions are necessary.
- Trend analyses show a reduction in traffic-related eBC, but an increase in biomass burning eBC. This shift underscores the need for stronger measures to reduce emissions from agricultural and domestic solid fuel combustion.

- Implementing targeted measurements and source apportionment tools is essential to distinguish between the two main eBC sub-fractions (i.e., liquid vs. solid fuel burning emissions) enabling cost-effective abatement strategies. Appropriated eBC source apportionment approaches are given in RI-Urbans ST11 guidance document.

8 REFERENCES

ACTRIS-ECAC 2016. Intercomparison of Absorption Photometers Project No.: AP---2016---1---3. www.actris-ecac.eu/files/ECAC_report-AP-2016-1-3_the-cyprus-institute_AE31-1050-1009.pdf

Asmi, E., Backman, J., Servomaa, H., Virkkula, A., Gini, M.I., Eleftheriadis, K., Müller, T., Ohata, S., Kondo, Y., Hyvärinen, A., 2021. Absorption instruments inter-comparison campaign at the Arctic Pallas station. Atmos. Meas. Tech. 14, 5397–5413. https://doi.org/10.5194/amt-14-5397-2021

Cavalli, F., Putaud, J.P., 2010. Toward a standardized thermal-optical protocol for measuring atmospheric organic and elemental carbon: The eusaar protocol. ACS, Div. Environ. Chem. - Prepr. Ext. Abstr. 48, 443–446.

Ciupek, K., Quincey, P., Green, D.C., Butterfield, D., Fuller, G.W., 2021. Challenges and policy implications of long-term changes in mass absorption cross-section derived from equivalent black carbon and elemental carbon measurements in London and south-east England in 2014-2019. Environ. Sci. Process. Impacts 23, 1949–1960. https://doi.org/10.1039/d1em00200g

Cuesta-Mosquera, A., Mocnik, G., Drinovec, L., Müller, T., Pfeifer, S., Minguillon, M.C., Briel, B., Buckley, P., Dudoitis, V., Fernández-García, J., Fernandez-Amado, M., De Brito, J.F., Riffault, V., Flentje, H., Heffernan, E., Kalivitis, N., Kalogridis, A.C., Keernik, H., Marmureanu, L., Luoma, K., Marinoni, A., Pikridas, M., Schauer, G., Serfozo, N., Servomaa, H., Titos, G., Yus-Diez, J., Zioła, N., Wiedensohler, A., 2021. Intercomparison and characterization of 23 Aethalometers under laboratory and ambient air conditions: Procedures and unit-to-unit variabilities. Atmos. Meas. Tech. 14, 3195–3216. https://doi.org/10.5194/amt-14-3195-2021

Drinovec, L., Gregoric, A., Zotter, P., Wolf, R., Anne Bruns, E., Bruns, E.A., Prevot, A.S.H., Favez, O., Sciare, J., Arnold, I.J., Chakrabarty, R.K., Moosmüller, H., Filep, A., Mocnik, G., 2017. The filter-loading effect by ambient aerosols in filter absorption photometers depends on the coating of the sampled particles. Atmos. Meas. Tech. 10, 1043–1059. https://doi.org/10.5194/amt-10-1043-2017

Drinovec, L., Močnik, G., Zotter, P., Prévôt, A.S.H., Ruckstuhl, C., Coz, E., Rupakheti, M., Sciare, J., Müller, T., Wiedensohler, A., Hansen, A.D.A., 2015. The "dual-spot" Aethalometer: An improved measurement of aerosol black carbon with real-time loading compensation. Atmos. Meas. Tech. 8, 1965–1979. https://doi.org/10.5194/amt-8-1965-2015

EN12341:2023 'Ambient Air — Standard gravimetric measurement method for the determination of the PM10 or PM2.5 mass concentration of suspended particulate matter', CEN, Brussels.

EN16909:2017. European Committee for Standardisation (CEN), Ambient Air Measurement of Elemental Carbon (EC) and Organic Carbon (OC) Collected on Filters, CEN, Brussels.

Helin, A., Niemi, J. V., Virkkula, A., Pirjola, L., Teinilä, K., Backman, J., Aurela, M., Saarikoski, S., Rönkkö, T., Asmi, E., Timonen, H., 2018. Characteristics and source apportionment of black carbon in the Helsinki metropolitan area, Finland. Atmos. Environ. 190, 87–98. https://doi.org/10.1016/j.atmosenv.2018.07.022

Grange, S.K., Lötscher, H., Fischer, A., Emmenegger, L., Hueglin, C., 2020. Evaluation of equivalent black carbon source apportionment using observations from Switzerland between 2008 and 2018. Atmos. Meas. Tech. 13, 1867–1885. https://doi.org/10.5194/amt-13-1867-2020

Karanasiou, A., Minguillón, M.C., Viana, M., Alastuey, A., Putaud, J.-P., Maenhaut, W., Panteliadis, P., Močnik, G., Favez, O., Kuhlbusch, T.A.J., 2015. Thermal-optical analysis for the measurement of elemental carbon (EC) and organic carbon (OC) in ambient air a literature review. Atmos. Meas. Tech. Discuss 8, 9649–9712. https://doi.org/10.5194/amtd-8-9649-2015

Karanasiou, A., Panteliadis, P., Perez, N., Minguillón, M.C., Pandolfi, M., Titos, G., Viana, M., Moreno, T., Querol, X., Alastuey, A., 2020. Evaluation of the Semi-Continuous OCEC analyzer performance with the EUSAAR2 protocol. Sci. Total Environ. 747. https://doi.org/10.1016/j.scitotenv.2020.141266

Mbengue, S., Zikova, N., Schwarz, J., Vodička, P., Šmejkalová, A.H., Holoubek, I., 2021. Mass absorption cross-section and absorption enhancement from long term black and elemental carbon measurements: A rural background station in Central Europe. Sci. Total Environ. 794. https://doi.org/10.1016/j.scitotenv.2021.148365

Müller, T., Fiebig, M., 2018. ACTRIS In Situ Aerosol: Guidelines for Manual QC of AE33 absorption photometer data. https://www.actris-ecac.eu/ (accessed 2.4.24).

Müller, T., Henzing, J.S., De Leeuw, G., Wiedensohler, A., Alastuey, A., Angelov, H., Bizjak, M., Collaud Coen, M., Engström, J.E., Gruening, C., Hillamo, R., Hoffer, A., Imre, K., Ivanow, P., Jennings, G., Sun, J.Y., Kalivitis, N., Karlsson, H., Komppula, M., Laj, P., Li, S.M., Lunder, C., Marinoni, A., Martins Dos Santos, S., Moerman, M., Nowak, A., Ogren, J.A., Petzold, A., Pichon, J.M., Rodriquez, S., Sharma, S., Sheridan, P.J., Teinilä, K., Tuch, T., Viana, M., Virkkula, A., Weingartner, E., Wilhelm, R., Wang, Y.Q., 2011. Characterization and intercomparison of aerosol absorption photometers: Result of two intercomparison workshops. Atmos. Meas. Tech. 4, 245–268. https://doi.org/10.5194/amt-4-245-2011

Petzold, A., Ogren, J.A., Fiebig, M., Laj, P., Li, S.M., Baltensperger, U., Holzer-Popp, T., Kinne, S., Pappalardo, G., Sugimoto, N., Wehrli, C., Wiedensohler, A., Zhang, X.Y., 2013. Recommendations for reporting black carbon measurements. Atmos. Chem. Phys. 13, 8365–8379. https://doi.org/10.5194/acp-13-8365-2013

Petzold, A., Schloesser, H., Sheridan, P.J., Arnott, W.P., Ogren, J.A., Virkkula, A., 2005. Evaluation of multiangle absorption photometry for measuring aerosol light absorption. Aerosol Sci. Technol. 39, 40–51. https://doi.org/10.1080/027868290901945

Petzold, A., Schönlinner, M., 2004. Multi-angle absorption photometry - A new method for the measurement of aerosol light absorption and atmospheric black carbon. J. Aerosol Sci. 35, 421–441. https://doi.org/10.1016/j.jaerosci.2003.09.005

Rigler, M., Drinovec, L., Lavri, G., Vlachou, A., Prevot, A.S.H., Luc Jaffrezo, J., Stavroulas, I., Sciare, J., Burger, J., Kranjc, I., Turšič, J., D. A. Hansen, A., Mocnik, G., 2020. The new instrument using a TC-BC (total carbon-black carbon) method for the online measurement of carbonaceous aerosols. Atmos. Meas. Tech. 13, 4333–4351. https://doi.org/10.5194/amt-13-4333-2020

Sandradewi, J., Prévôt, A.S.H., Szidat, S., Perron, N., Alfarra, M.R., Lanz, V.A., Weingartner, E., Baltensperger, U.R.S., 2008. Using aerosol light abosrption measurements for the quantitative determination of wood burning and traffic emission contribution to particulate matter. Environ. Sci. Technol. 42, 3316–3323. https://doi.org/10.1021/es702253m

Savadkoohi, M., Pandolfi, M., Favez, O., Putaud, J., Eleftheriadis, K., Fiebig, M., Hopke, P.K., Laj, P., Wiedensohler, A., Alados-arboledas, L., Bastian, S., Chazeau, B., María, C., Colombi, C., Costabile, F., Green, D.C., Hueglin, C., Liakakou, E., Luoma, K., Listrani, S., Mihalopoulos, N., Petit, J., Rattigan, O. V, Reche, C., Timonen, H., Titos, G., Tremper, A.H., Vratolis, S., Vodi, P., Yubero, E., Harrison, R.M., Pet, T., Querol, X., 2024. Recommendations for reporting equivalent black carbon (eBC) mass concentrations based on long-term pan-European in-situ observations. Environ. Int. 185. https://doi.org/10.1016/j.envint.2024.108553

Savadkoohi, M., Pandolfi, M., Reche, C., Niemi, J. V, Mooibroek, D., Titos, G., Green, D.C., Tremper, A.H., Hueglin, C., Coz, E., Liakakou, E., Mihalopoulos, N., Stavroulas, I., Alados-arboledas, L., Beddows, D., Brito, J.F. De, Bastian, S., Baudic, A., Colombi, C., Costabile, F., Estell, V., Matos, V., Gaag, E. Van Der, Norman, M., Silvergren, S., Petit, J., Putaud, J., Rattigan, O. V, Timonen, H., Tuch, T., Merkel, M., Weinhold, K., Vratolis, S., Vasilescu, J., Favez, O., Harrison, R.M., Laj, P., Wiedensohler, A., Hopke, P.K., Pet, T., Querol, X., 2023. The variability of mass concentrations and source apportionment analysis of equivalent black carbon across urban Europe. Environ. Int. J. 178. https://doi.org/10.1016/j.envint.2023.108081

Segura, S., Estellés, V., Titos, G., Lyamani, H., Utrillas, M.P., Zotter, P., Prévôt, A.S.H., Močnik, G., Alados-Arboledas, L., Martínez-Lozano, J.A., 2014. Determination and analysis of in situ spectral aerosol optical properties by a multi-instrumental approach. Atmos. Meas. Tech. 7, 2373–2387. https://doi.org/10.5194/amt-7-2373-2014

Srivastava, P., Naja, M., Seshadri, T.R., Joshi, H., Dumka, U.C., Gogoi, M.M., Babu, S.S., 2022. Implications of Site-specific Mass Absorption Cross-section (MAC) to Black Carbon Observations at a High-altitude Site in the Central Himalaya. Asia-Pacific J. Atmos. Sci. 58, 83–96. https://doi.org/10.1007/s13143-021-00241-6

Valentini, S., Bernardoni, V., Bolzacchini, E., Ciniglia, D., Ferrero, L., Forello, A.C., Massabó, D., Pandolfi, M., Prati, P., Soldan, F., Valli, G., Yus-Díez, J., Alastuey, A., Vecchi, R., 2021. Applicability of benchtop multi-wavelength

polar photometers to off-line measurements of the Multi-Angle Absorption Photometer (MAAP) samples. J. Aerosol Sci. 152, 1–13. https://doi.org/10.1016/j.jaerosci.2020.105701

Virkkula, A., Mäkelä, T., Hillamo, R., Yli-Tuomi, T., Hirsikko, A., Hämeri, K., Koponen, I.K., 2007. A simple procedure for correcting loading effects of aethalometer data. J. Air Waste Manag. Assoc. 57, 1214–1222. https://doi.org/10.3155/1047-3289.57.10.1214

Weingartner, E., Saathoff, H., Schnaiter, M., Streit, N., Bitnar, B., Baltensperger, U., 2003. Absorption of light by soot particles: Determination of the absorption coefficient by means of aethalometers. J. Aerosol Sci. 34, 1445–1463. https://doi.org/10.1016/S0021-8502(03)00359-8

Wu, L., Wu, C., Deng, T., Wu, D., Li, M., Li, Y. J., and Zhou, Z., 2024. Field comparison of dual- and single-spot Aethalometers: equivalent black carbon, light absorption, Ångström exponent and secondary brown carbon estimations, Atmos. Meas. Tech., 17, 2917–2936, https://doi.org/10.5194/amt-17-2917-20244.

Yus-Díez, J., Bernardoni, V., Močnik, G., Alastuey, A., Ciniglia, D., Ivančič, M., Querol, X., Perez, N., Reche, C., Rigler, M., Vecchi, R., Valentini, S., Pandolfi, M., 2021. Determination of the multiple-scattering correction factor and its cross-sensitivity to scattering and wavelength dependence for different AE33 Aethalometer filter tapes: a multi-instrumental approach. Atmos. Meas. Tech. Discuss. 14, 6335–6355. https://doi.org/10.5194/amt-2021-46

Zanatta, M., Gysel, M., Bukowiecki, N., Müller, T., Weingartner, E., Areskoug, H., Fiebig, M., Yttri, K.E., Mihalopoulos, N., Kouvarakis, G., Beddows, D., Harrison, R.M., Cavalli, F., Putaud, J.P., Spindler, G., Wiedensohler, A., Alastuey, A., Pandolfi, M., Sellegri, K., Swietlicki, E., Jaffrezo, J.L., Baltensperger, U., Laj, P., 2016. A European aerosol phenomenology-5: Climatology of black carbon optical properties at 9 regional background sites across Europe. Atmos. Environ. 145, 346–364. https://doi.org/10.1016/j.atmosenv.2016.09.035

Zotter, P., Herich, H., Gysel, M., El-Haddad, I., Zhang, Y., Mocnik, G., Hüglin, C., Baltensperger, U., Szidat, S., Prévôt, A.S.H., 2017. Evaluation of the absorption Ångström exponents for traffic and wood burning in the Aethalometer-based source apportionment using radiocarbon measurements of ambient aerosol. Atmos. Chem. Phys. 17, 4229–4249. https://doi.org/10.5194/acp-17-4229-2017